Importance of structural history in the summit area of Stromboli during the 2002–2003 eruptive crisis inferred from temperature, soil CO2, self-potential, and electrical resistivity tomography

Anthony Finizola, Maurice Aubert, André Revil, Claudia Schütze, Francesco Sortino

Importance of structural history in the summit area of Stromboli during the 2002–2003 eruptive crisis inferred from temperature, soil CO_2, self-potential, and electrical resistivity tomography

Anthony Finizola [a,*], Maurice Aubert [b], André Revil [c,d], Claudia Schütze [e], Francesco Sortino [f]

[a] Laboratoire GéoSciences Réunion, Université de La Réunion, Institut de Physique du Globe de Paris, CNRS, UMR 7154-Géologie des Systèmes Volcaniques, 15 avenue René Cassin, BP 7151, 97715 Saint Denis cedex 9, La Réunion, France
[b] Laboratoire Magmas et Volcans, Clermont-Université, UMR 6524, CNRS, 5 rue Kessler, 63038 Clermont-Ferrand, France
[c] Colorado School of Mines, Green Center, Dept of Geophysics, 1500 Illinois Street, Golden, CO, 80401-1887, USA
[d] LGIT, UMR 5559, CNRS, Equipe Volcan, Université de Savoie, 73376 Le Bourget-du-lac Cedex, France
[e] Department of Geophysics and Geology, Universität Leipzig, Talstr. 35, D-04103 Leipzig, Germany
[f] Istituto Nazionale di Geofisica e Vulcanologia, Sezione di Palermo, Via Ugo La Malfa, 153, 90146 Palermo, Italy

A B S T R A C T

The 2002–2003 eruptive crisis of Stromboli volcano in the Aeolian Islands raised the question of how to assess the stability of the flanks of this volcanic edifice during such a crisis. To provide a response to this question, we analyzed a detailed fluid flow mapping plus the reiteration of a profile located in the vicinity of the active vents using the self-potential method, temperature data, soil-gas (CO_2) measurements, and electric resistivity tomography. Coupling the interpretation of these methods that are sensitive to the flow of gas and water in the ground indicates the position of areas of mechanical weakness. In addition, they can be used to monitor the change in the discharge of fluids associated with these features before and during the 2002–2003 eruptive crisis. Our results emphasize the importance of old structural boundaries, such as the Large Fossa crater, in the development of the new set of fractures observed during the 2002–2003 eruptive crisis. Between October 2002 and January 2003, the use of CO_2 soil-gas technique evidenced an increase in the discharge of CO_2 outside the Large Fossa crater boundaries, along the failure boundary of the southern Sciara del Fuoco area. Self-potential and temperature measurements made before the 2002–2003 eruptive crisis reveal significant changes along the main structural boundaries of the Fossa area. The development of these anomalies is interpreted as an increase of the permeability of the structure from May 2000 to May 2002. Between January 2003 and March 2003 the reiteration of self-potential, temperature, and CO_2 measurements shows an increase of fluid discharge along weakness planes located inside the Large Fossa crater boundary. They evidence no change outside this structural boundary. The importance of the Large Fossa crater boundary in controlling the deformation and fluid flow from January to March 2003 has been attested by the development of the fractures inside the Large Fossa crater boundary, and also with a network of electrooptical distance measurement stations located inside and outside this ancient crater. This multidisciplinary approach to fluid flow assessment before and during an eruptive crisis is complementary to geodetic measurements of the deformation of the edifice. It demonstrates for the first time the powerful potential of combining electrical resistivity tomography, self-potential, temperature, and soil CO_2 measurements in assessing the position of the planes of mechanical weakness in a volcanic edifice.

1. Introduction

Stromboli is a small volcanic island located in the Tyrrhenian Sea, in the northernmost part of the Aeolian archipelago. Its altitude is 924 m above the sea level high and ~3400 m above the sea floor. The structural and magmatological evolution of the emerged part of this island has been subdivided by Hornig-Kjarsgaard et al. (1993) in seven major periods separated by one erosional period, four caldera collapses, and one crater and flank collapse episode. During the last one thousand years, the eruptive activity of Stromboli was mainly characterized by a mild persistent rhythmic explosive activity that has been used to defined the so-called "strombolian eruptive style". This activity is sometimes disrupted by both lava flows and major explosive events (Barberi et al., 1993; Rosi et al., 2000). During the strongest explosive events, called paroxysmal events, an interaction between

* Corresponding author. Tel.: +33 262 262 93 82 06; fax: +33 262 262 93 82 66.
E-mail address: anthony.finizola@univ-reunion.fr (A. Finizola).

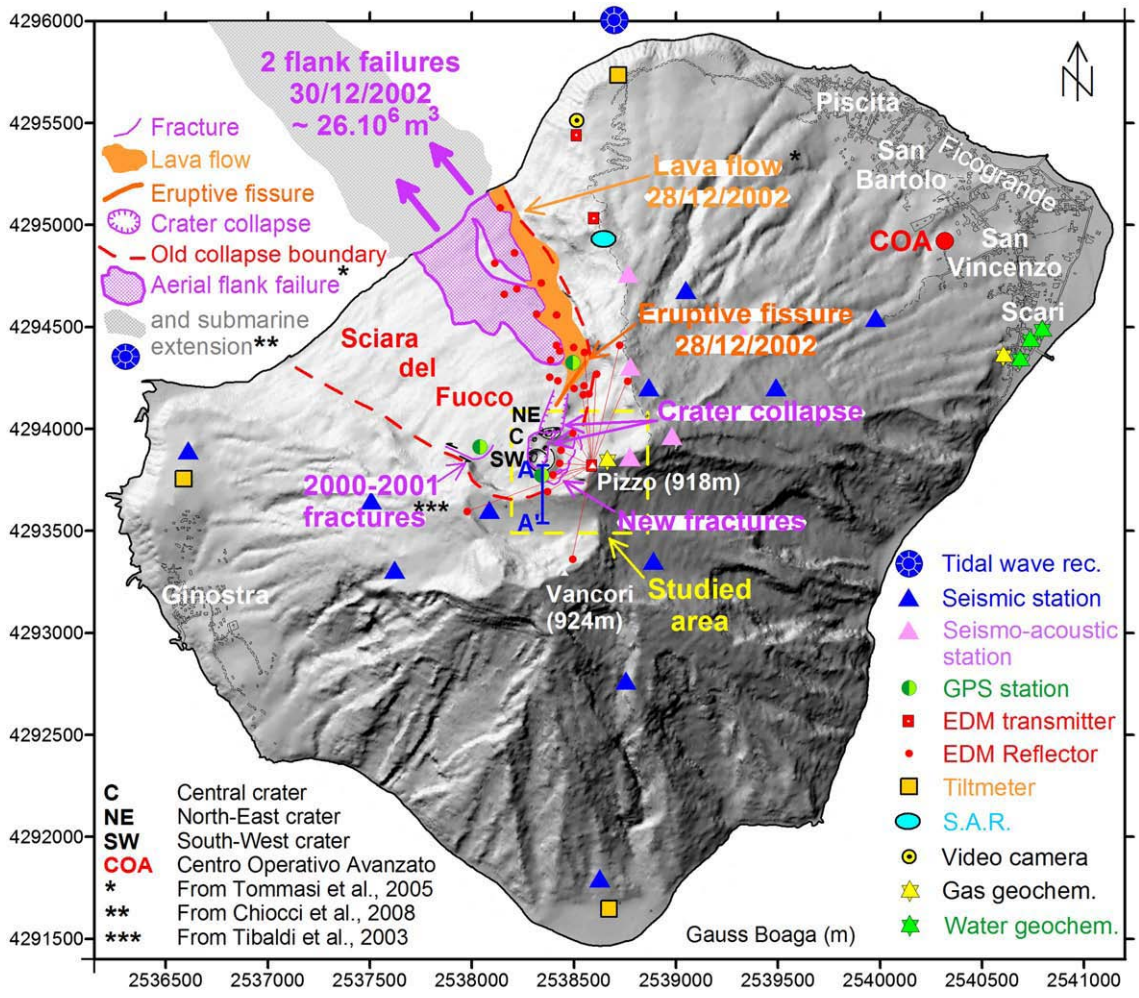

Fig. 1. Map of Stromboli Island showing the effusive and collapse events that occurred at the beginning of the 2002–2003 eruptive crisis and the position of the monitoring network. This network was set up at the beginning of the eruptive crisis by the Italian volcanologists to assess the stability of the Sciara del Fuoco sector collapse area. This network comprised various scientific instruments located over the island. The Profile A–A′ located in the upper central part of the volcano corresponds to a reiterated profiled in terms of self-potential, temperature, and soil-gas measurements. It stands along a north–south direction crossing the Sciara del Fuoco sector collapse, the Pizzo crater, the Large Fossa crater, and the SW crater boundaries.

magma and water has been suggested by Rittmann (1931) (see also Bertagnini and Landi, 1996; Bonaccorso et al., 2003; Revil et al., 2004; Finizola et al., 2006; Porreca et al., 2006).

On December 28th 2002, an important volcanic crisis began at Stromboli. It involved important changes in the eruptive activity and also in the morphology of the edifice (Bonaccorso et al., 2003; Calvari et al., 2005, 2006, and Fig. 1). On December 28th, 2002, lava was emitted from an eruptive fissure located in the northern part of the Sciara del Fuoco area. This event was associated with the partial collapse of the external northern flank of the NE crater (Figs. 1 and 2). Two days later, on December 30th, 2002, two landslides occurred with a total volume estimated to $\sim 26 \times 10^6$ m^3 (Bonaccorso et al., 2003; Baldi et al., 2005; Tommasi et al., 2005; Chiocci et al., 2008). These landslides were responsible for two small tsunamis, which damaged several houses in the villages of Piscità, Ficogrande, and Scari (Maramai et al., 2005) (see their positions in Fig. 1). During the seven following months, the aerial part of these collapses was quickly refilled by the persistent effusive activity of the volcano. This effusive activity stopped on July 22nd, 2003 (Calvari et al., 2005). This eruptive crisis was also characterized by a centripetal deformation associated with the collapse of the summit craters, at the junction of the Central and NE craters and the partial collapse of the SW crater (see their position in Fig. 2). During this period, a network of open fractures appeared in the summit of the edifice cutting all the Fossa area. Some of these fractures were associated with the emission of fumaroles. The horizontal and vertical displacements of these fractures reached maximum amplitude of 15 to 20 cm, respectively, at some points.

Appearing at the beginning of the eruptive crisis, the occurrence of these different collapses and the formation of a network of open fractures brought some legitimate concerns about the stability of the Sciara del Fuoco flank of the edifice (see Fig. 1). In particular, a dramatic scenario would have been the reactivation of the sliding plane of the entire aerial and submarine Sciara del Fuoco sector collapse area (Fig. 1). Such a flank collapse may have mobilized a volume of about 1 km^3 according to Tibaldi (2001). This is approximately fifty times the volume that was involved in the flank collapses that occurred at the beginning of the eruptive crisis and that were responsible for the two small tsunami described above. The consequence of such a catastrophic collapse scenario would be an important tsunami (likely more than 10 m in amplitude), which would have severely impacted the coastland of Stromboli, the whole Aeolian Archipelago, and the Sicilian and Calabrian shores as well (Tinti et al., 2003).

To provide a suitable response to this potential geohazard, an important monitoring network was quickly developed by volcanologists and the Italian Civil Protection Institute. Fig. 1 shows the different permanent monitoring stations installed at the beginning of the crisis, including a Global Positioning System (GPS) network, an

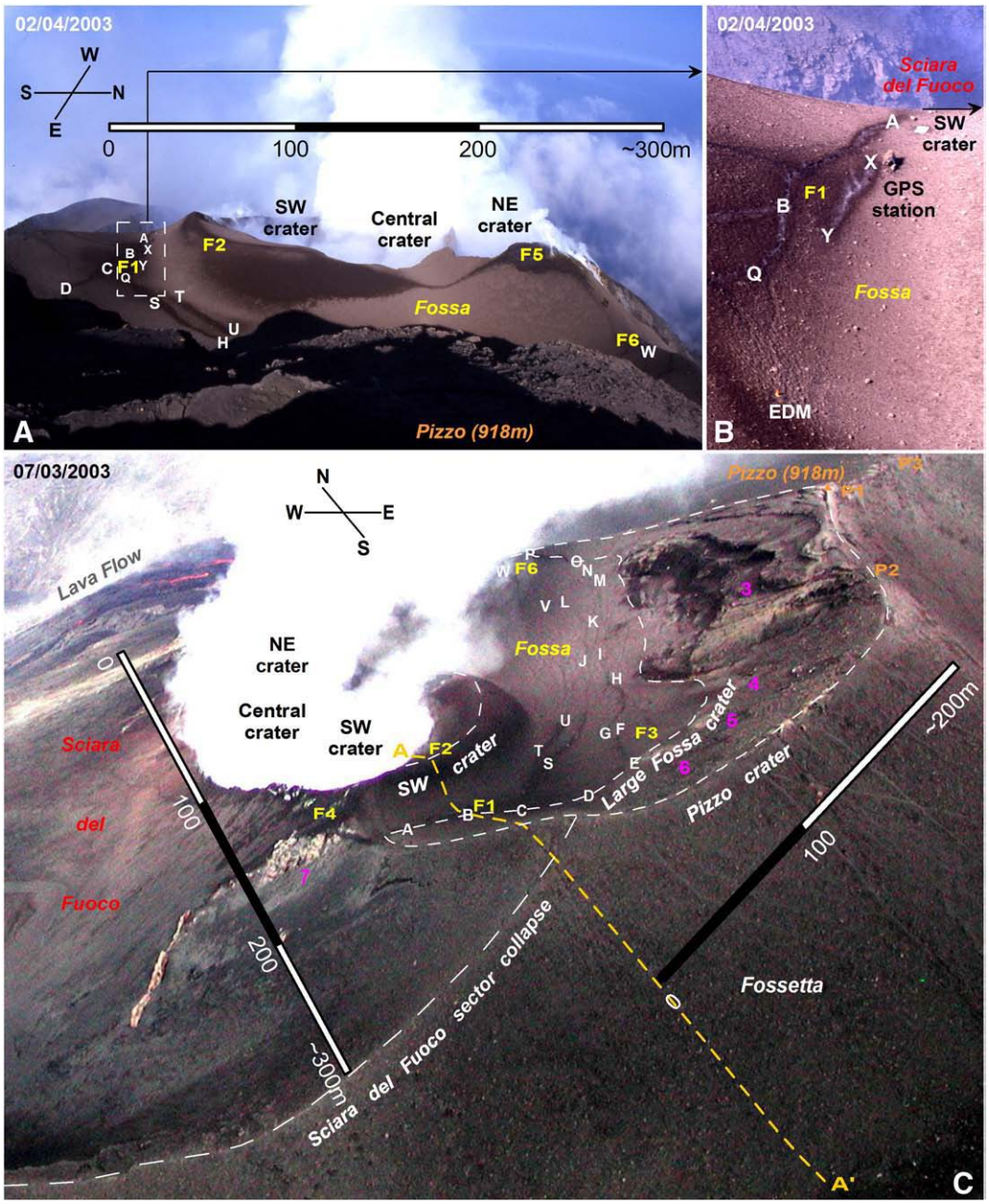

Fig. 2. Pictures showing the position of the network of new fractures in the summit part of Stromboli at the beginning of the 2002–2003 eruptive crisis. F1 to F6 and P1 to P3 represent the maxima of the thermal anomalies located in the Fossa and Pizzo areas, respectively. The labels of the fractures are discussed in the main text. A: View of the Fossa area with the three active craters. B: Details of the southern part of SW crater in the Fossa area. C: Aerial view of the summit part of Stromboli volcano showing the Pizzo area, the Fossa area, the three active craters, the Fossetta area, and the Sciara del Fuoco area where the active lava flow took place. Profile A–A′ is shown as in Fig. 1.

Electrooptical Distance Measurement (EDM) network, and a Synthetic Aperture Radar (SAR). It was also time to realize all the data that were available in this area. Since 1994, Finizola and co-workers performed a multidisciplinary study at Stromboli involving high resolution electrical resistivity tomography, self-potential, temperature, and soil-gas (CO_2) measurements. These surveys were performed to study the pattern of ground water flow in the summit crater area of Stromboli (Finizola et al., 2003; Revil et al., 2004). In addition to these high resolution measurements, other measurements were performed with the same set of methods at the scale of the whole island (Finizola et al., 2002, 2006). Finizola et al. (2002) identified the presence of a hydrothermal system intersected by two regional faults. In the summit (Fossa-Pizzo) area, close to the active vents, self-potential, temperature, and soil CO_2 measurements revealed anomalies related to the uprising of hydrothermal fluids along faults bordering the rims of the present-day active craters (especially the NE and SW craters). They also identified additional anomalies associated with the boundaries of two older craters called the Large Fossa crater and the Pizzo crater (Finizola et al., 2003; Revil et al., 2004). Moreover, in the summit area, a profile entering inside the SW crater was reiterated five times since 1994 with some of the above-mentioned techniques. In January, March, and April 2003, we carried out a campaign of self-potential, temperature, and soil CO_2 measurements at Stromboli volcano to assess the changes of fluid flow associated with the 2002–2003 eruptive crisis.

The goal of the present study is to test the sensitivity of the above-mentioned set of methods (self-potential, temperature, and soil CO_2 concentration measurements) to monitor the network of fractures

that appeared in the summit area of the volcano at the beginning of the eruptive crisis (Figs. 1 and 2). All these data were analyzed to provide a precise comparison of the fluid flow dynamics before and during the eruptive crisis in order to provides responses to the following questions: (1) What is the cause of the network of fractures observed in the summit part of the volcano? (2) What is the sensitivity of geophysical methods to changes in the fluid flow dynamics observed in the summit area before and during the eruptive crisis? The responses to these questions provide a better assessment of the geohazard associated with the stability of the NW flank of Stromboli.

2. Methods

In this section, we provide a short description of the three different techniques (self-potential, temperature, and soil-gas) used in this study.

2.1. Self-potential measurements

The self-potential method consists in measuring passively the distribution of natural electrical potential at the ground surface of the Earth with a high-input impedance voltmeter and a pair of non-polarizing electrodes. In a volcanic context, this electrical potential represents the signature of ground water flow and the shape of the equipotentials is influenced by the distribution of the electrical resistivity of the ground. The flow of ground water itself is controlled, in steady state conditions, by the distribution of the permeability, the capillary pressure and relative permeability curves, and the distribution of the pressure of the water phase. There is generally a positive excess of charge in the pore water to compensate the negative charge on the mineral surface (Revil and Leroy, 2001). However, recent laboratory experiments demonstrated that, in some cases, the charge of the pore water can be negative to compensate a positive charge on the mineral surface (Hase et al., 2003; Guichet et al., 2006; Aizawa et al., 2008). This is however not the case at Stromboli (Revil et al., 2004).

The flow of water drags charges of the pore water and therefore produces an electrical current (Revil et al., 1999a,b; Lorne et al., 1999a,b; Revil et al., 2003a,b; Ishido, 2004). Self-potential is used on active volcanoes to identify the uprising of hot hydrothermal fluids for instance (Zablocki, 1976; Aubert and Kieffer, 1984; Aubert et al., 1984; Aubert and Lima, 1986; Aubert and Baubron, 1988; Malengreau et al., 1994; Lénat et al., 1998; Finizola et al., 2002, 2003, 2004).

Revil and Linde (2006) have developed a new theory of electrokinetic effects based on the excess of charge per unit volume rather than on the zeta potential. When the pH of the pore water is close to 7 ± 2, the theory can be associated with the fact that excess of charge per unit pore volume scales directly with the permeability, removing the need for additional (usually unknown) rock properties like in previous theoretical models. This theory has been generalized subsequently to unsaturated porous materials by Linde et al. (2007) and Revil et al. (2007) and to flow in the inertial laminar flow regime by Bolève et al. (2007) and Crespy et al. (2007). However, because the pH of the pore water can change substantially over space and time in the hydrothermal system of an active volcano, the interpretation of self-potential data requires additional information like temperature, CO_2 soil concentration, and resistivity data.

2.2. Temperature measurements

The supply of heat in the vicinity of active craters is often responsible for the occurrence of shallow advective thermal anomalies when water is present in the pore space of the rocks. If the temperature is above the boiling temperature of water (which depends on the pressure and the total dissolved content), water moves as hot steam mixed with various gases inside the hydrothermal system. Hot steam can condense near the ground surface, like at Stromboli, or produces locally fumaroles like at Vulcano Island.

At Stromboli, high temperature anomalies measured at several tens of centimetres deep show an excellent correlation with positive self-potential anomalies without fumarole or temperature anomalies directly at the ground surface (Ballestracci, 1982; Nishida and Tomiya, 1987; Aubert and Baubron, 1988; Matsushima et al., 1990; Aubert, 1999; Finizola et al., 2003; Lewicki et al., 2003). However, there are cases for which the upwelling of hydrothermal fluids, evidenced by temperature anomalies, does not correlate with self-potential anomalies at all (Matsushima et al., 1990; Zlotnicki and Nishida, 2003).

2.3. CO_2 soil-gas measurements

On active volcanoes, the exsolution of CO_2 from magma occurs at a depth of several kilometres. CO_2 rises to the surface through highly permeable zones, which may also drain other fluids like hot steam. It follows that these permeable areas (very often faults) are also associated with advective heat transport and therefore temperature anomalies. It follows that soil-gas anomalies and temperature anomalies over open cracks and faults show usually very good spatial correlations (Aubert and Baubron 1988; Finizola et al., 2003; Lewicki et al., 2003). Note that a change in the concentration of CO_2 can imply both a change in the magnitude of the source (exsolution of magma associated with new dike intrusion at depth) or a change in the permeability of the faults associated with hydromechanical disturbances. Both effects are difficult to deconvolve.

3. Data acquisition

During the 2002–2003 eruptive crisis, a detailed map of the network of fractures that occurred in the Fossa area was carried out in the mid of January, 2003. Such a survey was repeated in the beginning of April 2003 to check the possible development of this network (Fig. 3). Temperature and CO_2 soil-gas measurements were also mapped along the network of fractures with a take-out of 5 m.

Moreover, before the eruptive crisis, self-potential, temperature and CO_2 soil-gas measurements were performed along a N–S profile labelled A–A′ in Figs. 1, 2C and 3. These measurements were made in August 1994, August 1995, May 2000, May 2002, and October 2002. Reiterative profiles were carried out during the eruptive crisis in the mid of January 2003 and at the beginning of March 2003. These measurements were consistently taken at the same place by using wooden sticks installed every 5 m along Profile A–A′ of Fig. 1 since 1994 (see Finizola et al., 2003). Self-potential data was measured every meter, while temperature and CO_2 were measured every 2.5 m along Profile A–A′ (315 m long).

3.1. Self-potential measurements

The self-potential equipment consisted of a high internal impedance voltmeter (100 MΩ) with a sensitivity of 0.1 mV (Metrix, model MX20), a pair of non-polarizing $Cu/CuSO_4$ electrodes, and an insulated electric wire. The reference electrode was setup in the Fossetta area (point A′, see location in Figs. 2C and 3), 200 m away from the hydrothermal system of the Fossa area. The electrical contact with the ground was always very good (<90 kΩ for the contact resistance between the roving electrodes and the reference electrode). This is not surprising as evidence of moisture was indeed consistently found at a depth of few centimetres below the ground surface.

3.2. Temperature measurements

Thermal probes and a digital thermometer (Comark, model KM221) were used for the ground temperature measurements. Readings were

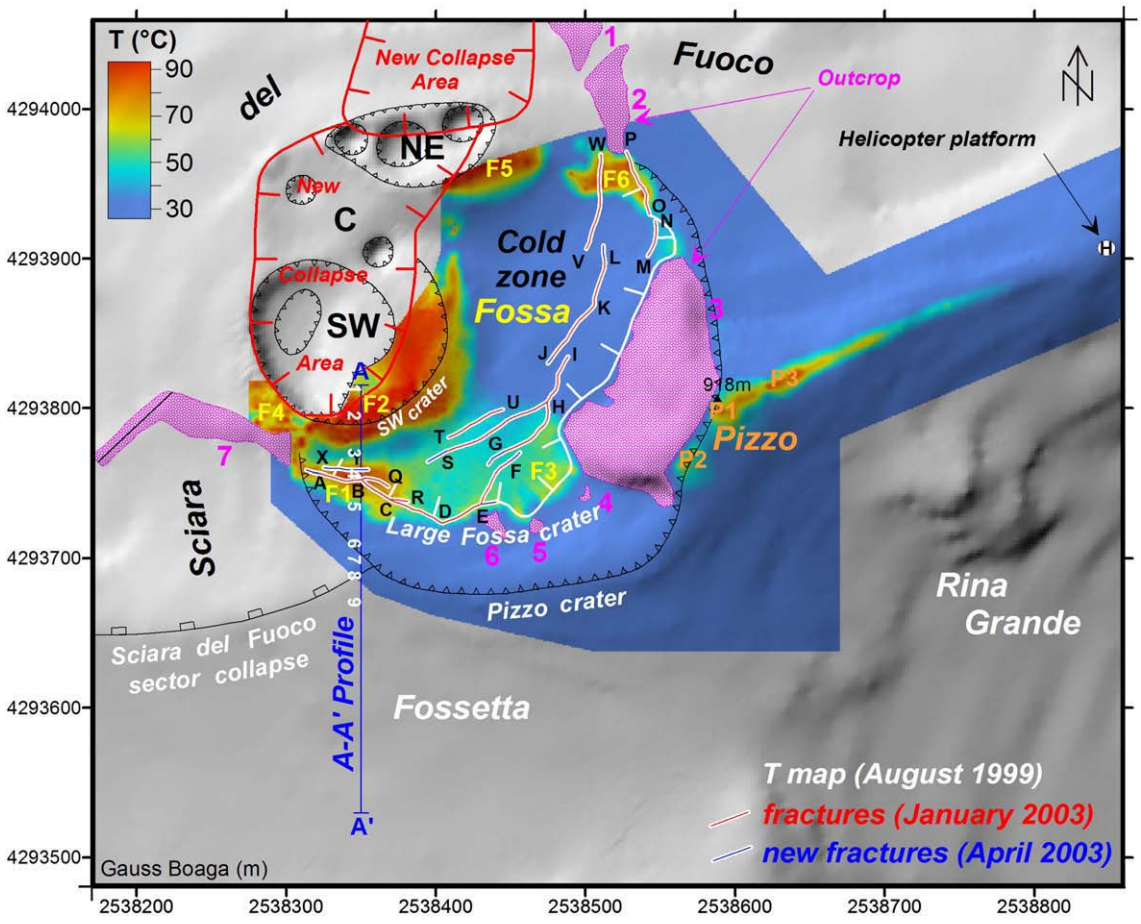

Fig. 3. Map of the set of fractures of January and April 2003 superimposed on the thermal map carried out in August 1999 and with the structural boundaries inferred by the self-potential, temperature, and the soil-gas measurements reported by Finizola et al. (2003). The labels F1–F6 and P1–P3 represent the maxima of the thermal anomalies detected in 1999 in the Fossa and Pizzo areas. The labels 1 to 7 (in pink) correspond to the position of the consolidated (mainly pyroclastics) outcrops. The labels 1 to 9 (in white) represent the different sectors of fluid flow identified along the A–A′ profile. They are also shown on Figs. 6 and 9 and commented in the text. (For interpretation of the references to color in this figure legend, the reader is referred to the web version of this article.)

taken to a tenth of degree Celsius. Each temperature measurement was taken by following four steps: (1) a small hole was dug to a precise depth of 30 cm with a steel rod, 2 cm in diameter, (2) then a thermal probe was inserted into the hole at a depth of 30 ± 1 cm by means of a graduated wooden stick, (3) the hole was compacted around the probe, and (4) a temperature reading was taken after 10–15 min in order to achieve thermal equilibrium.

3.3. Soil CO_2 measurements

In the field, it is possible to measure both the concentration of CO_2 in the vicinity of the ground surface or the flux of CO_2 through the ground surface. Etiope et al. (1999) demonstrated that a general linear relationship exists between the ground concentration and the flux of CO_2. On Stromboli volcano, the good correlation between CO_2 concentration and CO_2 flux was shown along the entire island by Finizola et al. (2006) and in the summit (Fossa) area (see a comparison between the data of Carapezza and Federico, 2000, and those of Finizola et al., 2003).

For practical reasons related to the weight, size, and electrical power of the equipment we choose to measure the concentration of CO_2 rather than the flux. We discuss later the limitations of this approach, especially in areas of high permeability draining high fluxes. To get reliable data of CO_2 concentration, gas was first pumped through a copper tube (2 mm in diameter), inserted in the soil to a depth of 0.5 m. The pumped gas was analysed directly in the field by infrared spectrometry (Edinburgh instruments, model GasCheck). The uncertainty is 5% in the concentration value.

4. Results

4.1. Location of the new fractures in the Fossa area

At the end of December 2002, at the beginning of the eruptive crisis, a network of fractures appeared in the Fossa area, around the SW, Central, and NE active craters (Figs. 1, 2, and 3). EDM reflectors and GPS stations were installed between these fractures and the active craters (Figs. 1 and 2B) to monitor their spatio-temporal evolution (Puglisi et al., 2005). A detailed map of the position of these fractures is compared with the map of the thermal anomalies observed in August 1999 by Finizola et al. (2003) in Fig. 3. This comparison allows distinguishing two kinds of fractures: (1) the first set corresponds to NW–SE oriented fractures. They are labelled A–B–C–D–E, B–Q, and C–R in Fig. 3. They perfectly superimposed on the maxima of the F1–F3 thermal anomalies identified in 1999 and associated with the border of the Large Fossa crater (Finizola et al., 2003). (2) A second set of fractures, roughly oriented NE–SW, is not related to previously defined thermal anomalies. They are labelled E–F, G–H–I, J–K–L, M–N, O–P, S–H, T–U, V–W in Fig. 3. The entire network of open fractures is located inside or along the structural boundary of the Large Fossa crater, along which fluids already migrated preferentially before the eruptive crisis (see the temperature anomalies labelled F1, F3, and F6 on Fig. 3 and in Finizola et al., 2003).

4.2. Fracturing in relation to temperature and CO_2 anomalies

Between the middle of January 2003 and the beginning of April 2003, we mapped the evolution of the network of fractures mentioned above. In less than three months, a lateral development of about 10 m of most of these fractures occurred (see the blue segments in positions E, F, G, J, and S in Fig. 3). A new fracture also appeared later and is labelled X–Y in Fig. 3.

A comparison between the temperature measured in August 1999 in the Fossa area (Figs. 4A and 5) and the temperature measured in January 2003 along the fractures (colour dots in Fig. 4A) shows a significant increase of the thermal activity in localized areas inside the structural boundary of the Large Fossa crater. These temperature changes, from August 1999 to January 2003, can be easier compared in Fig. 5 along the profile cutting the A–B–C–D–E–F–G–H–I–J–K–L–V–W set of fractures. In the southern part of the Fossa area, a temperature increase from 45–55 °C to more than 90 °C was observed, while in the northern part of the same area, the 'cold zone' defined in 1999 by Finizola et al. (2003) remained stable except for seasonal temperature variations between the summer 1999 and the winter 2003. Between

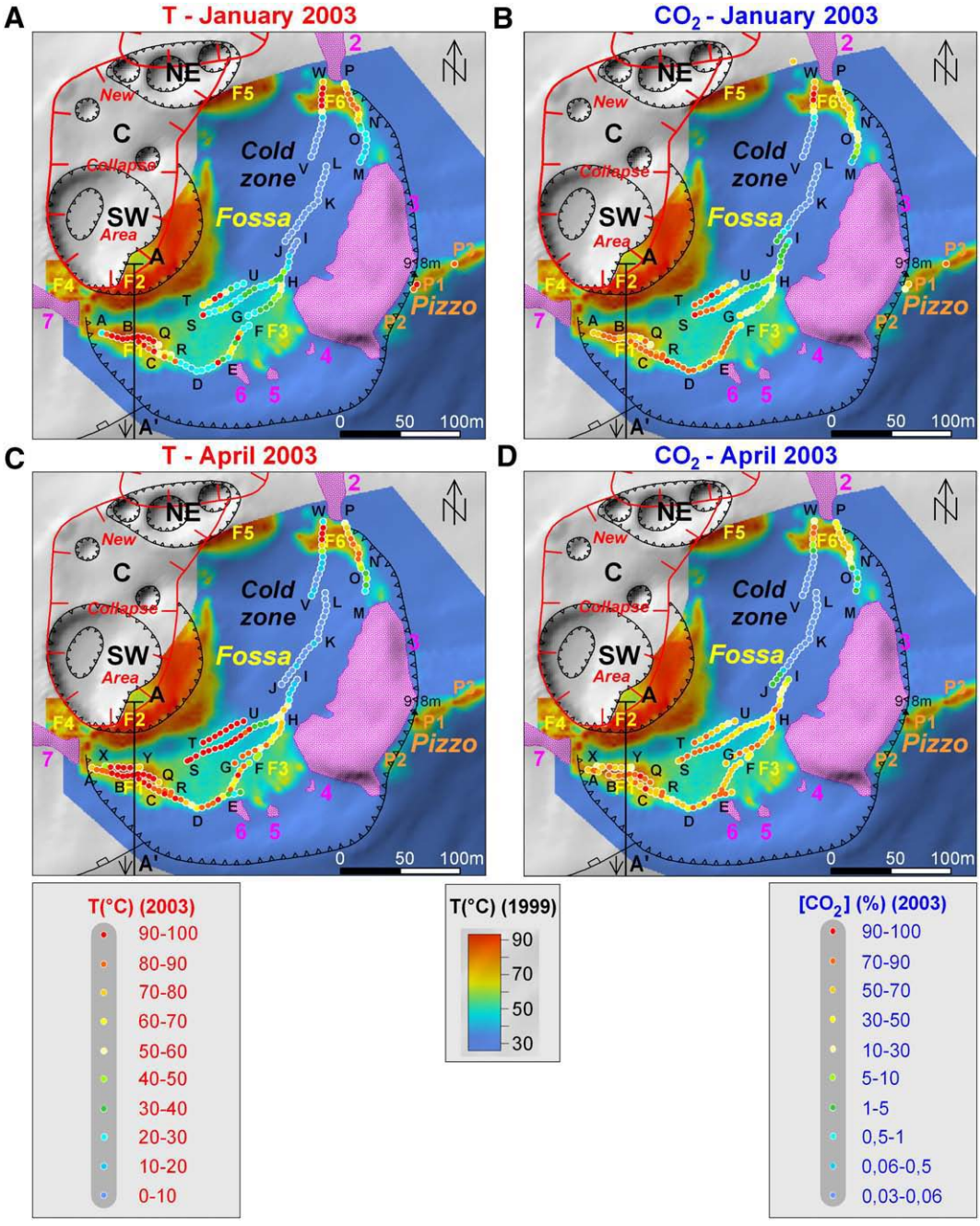

Fig. 4. Location of the stations where the temperature was measured at a depth of 30 cm and where the measurements of the concentration of CO_2 were performed (colored dots) along the network of open fractures in January and April 2003. This data are superimposed on the map of temperature data (at 30 cm) carried out in August 1999 (modified from Finizola et al., 2003). A: Temperature measurements in January 2003. B: Measurements of the concentration of CO_2 performed in January 2003. C: Temperature measurements performed in April 2003. D: measurements of the concentration of CO_2 performed in April 2003. Notations and symbols are the same as in Fig. 3. (For interpretation of the references to color in this figure legend, the reader is referred to the web version of this article.)

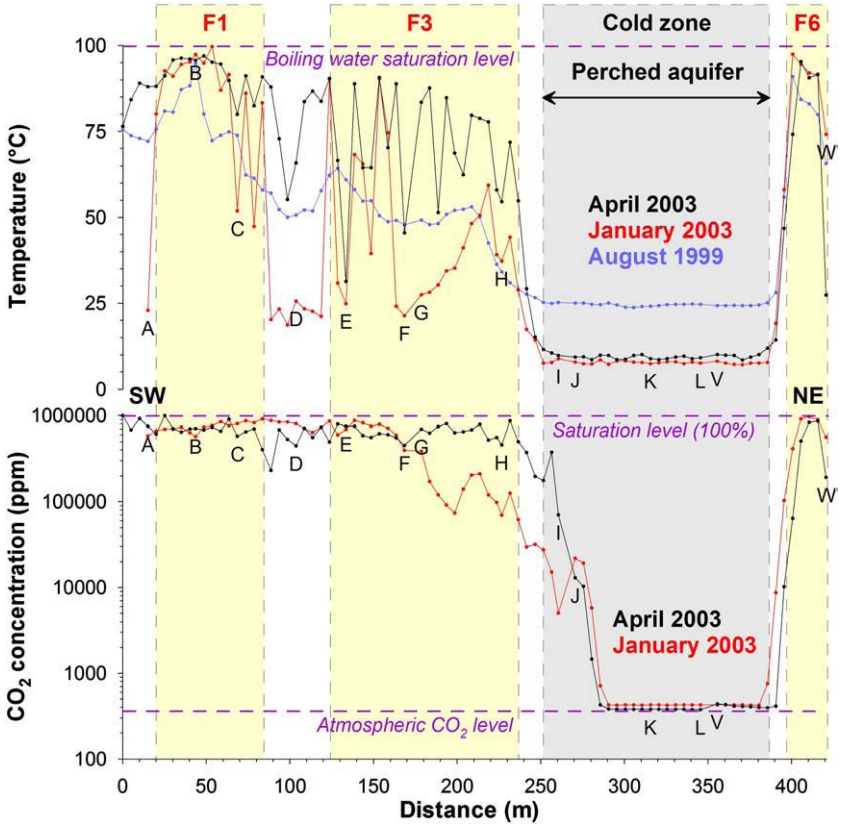

Fig. 5. Reiteration of temperature (at a depth of 30 cm) and CO_2 soil concentration measurements along the new fractures crossing the entire Fossa area in January and April 2003. Labels A to W allow locating this profile on Figs. 2, 3, and 4.

the middle of January 2003 (Figs. 4A and 5) and the beginning of April 2003 (Figs. 4C and 5), the temperature increased along several fractures in the southern part of the Fossa area (e.g. T–U and S–H in Fig. 4C), while temperature remained low (<25 °C) in the northern area.

The CO_2 soil concentrations measured along the fractures in the middle of January and at the beginning of April 2003 (Figs. 4B, D, and 5) display high values everywhere in the Fossa area except in the cold zone, which remained at the level of atmospheric values. This cold zone was interpreted by Finizola et al. (2003) and Revil et al. (2004) to be a perched aquifer. This aquifer is probably lying over a permeability barrier (seal) impeding the ascent of hydrothermal fluids (hot steam and CO_2) from below.

4.3. Self-potential, temperature, and CO_2 reiteration along Profile A–A′

Measurements of self-potential, temperature, and CO_2 soil concentration have repeatedly been recorded along Profile A–A′ since August 1994. This profile (see Figs. 2 and 3) was chosen to cross four fundamental structural boundaries, which preferentially channel the shallow fluid migration close to the active crater area. These boundaries are (1) the SW crater, (2) the Large Fossa crater, (3) the Pizzo crater, and (4) the Sciara del Fuoco sector collapse (Finizola et al., 2003; Revil et al., 2004). In order to simplify the description and interpretation of the profile A–A′, this profile has been subdivided into 9 sectors delineated according to the concentrations of CO_2 in the soil (Figs. 3 and 6): Sectors 2, 4, 6, and 8 correspond to high CO_2 concentrations. The intermediate sectors correspond to lower CO_2 concentrations.

4.3.1. Self-potential measurements

Self-potential measurements were reiterated from August 1995 to March 2003 along the profile A–A′. During this period, the self-potential data (Fig. 6) display no significant variation in the southern part of the profile (Sectors 5–9), outside the Large Fossa crater boundary. In contrast, in the northern part of the profile, a strong variation in the self-potential signal occurred especially in Sectors 4 and 2. This area was also associated with the temperature and CO_2 anomalies F1 and F2. In January 2003, the position of the maximum of the self-potential shifted by 12 m to the North from its original position in 1995 and 2000. There was therefore a striking superposition between self-potential, temperature, and CO_2 maxima on one hand and the position of the A–B fracture in the other of the 2002–2003 eruptive crisis (see Figs. 2, 3 and 6).

In March 2003, the measurements of the self-potential signals at the position of the F1 and F2 anomalies reached the highest values recorded during the whole survey. The self-potential signal increased by ~100 and 150 mV at the position of the anomalies F1 and F2, respectively, between May 2000 and March 2003. In Sector 2, the self-potential signals at the position of the F2 anomaly changed a local minimum during the period 1995–2000 to a maximum during the period 2002–2003. In Sector 1, we observed a decrease of self-potential signals from January to March 2003.

4.3.2. Temperature measurements

The anomalies F1 and F2 (Sectors 4 and 2 respectively in Fig. 6) display no significant changes in the maxima of the temperature before and during the eruptive crisis. At the opposite, the A–B fracture appeared in December 2002 exactly on the temperature maximum of the anomaly F1. Between January and March 2003, fracture X–Y was associated with an increase of the temperature, the self-potential, and the CO_2 soil concentration, as a consequence of faulting.

The temperature profiles also revealed a reduction of the width of the anomalies F1 and F2 between the periods 1994–1995 and 2002–2003. In addition, the temperature measured at the southern rim of Sector 2, from 1994 to 1995 is about 20–30 °C higher than the

temperature measured in 2002–2003. While the temperature recorded in the first period was measured in August (1994 and 1995) and the temperature in the second period were taken in January, March, and May, such a variation cannot be explained by seasonal variations alone, because soil temperature reached temperature higher than in the atmosphere (about 50 °C). This aspect will be discussed further below.

During the eruptive crisis, Sector 1 showed a twenty degree decrease of the temperature. In the cold areas (Sectors 6, 7, 8, and 9), outside the F1 and F2 fluid rising systems, a decrease of temperature of about 15 °C was observed. The decrease of about 15 °C in the cold Sectors 6, 7, 8, and 9 can be explained by seasonal variations of the ground surface temperature. However, the decrease of more that 20 °C in Sector 1 implies to consider changes of other parameters.

4.3.3. Soil CO_2 measurements

The main changes in the soil concentration of CO_2 occurred in Sector 7 (see Figs. 3 and 6). In October 2002, before the eruptive crisis, two distinct CO_2 peaks were identified and related to the Sciara del Fuoco sector collapse boundary (Sector 8) and to the rim of the Pizzo crater, respectively (Sector 6). These two peaks were separated by very low values of the CO_2 concentrations. This was a signature of preferential gas migrations along these two structural boundaries. In January 2003, a sharp increase in the concentrations of CO_2 occurred between these two structural boundaries, connecting the two previous anomalies in forming only one wide CO_2 concentration anomaly. The data of March 2003 display a general decrease of the CO_2 concentration along the entire profile. However, no important variations have been detected at the top of the F1 and F2 anomalies.

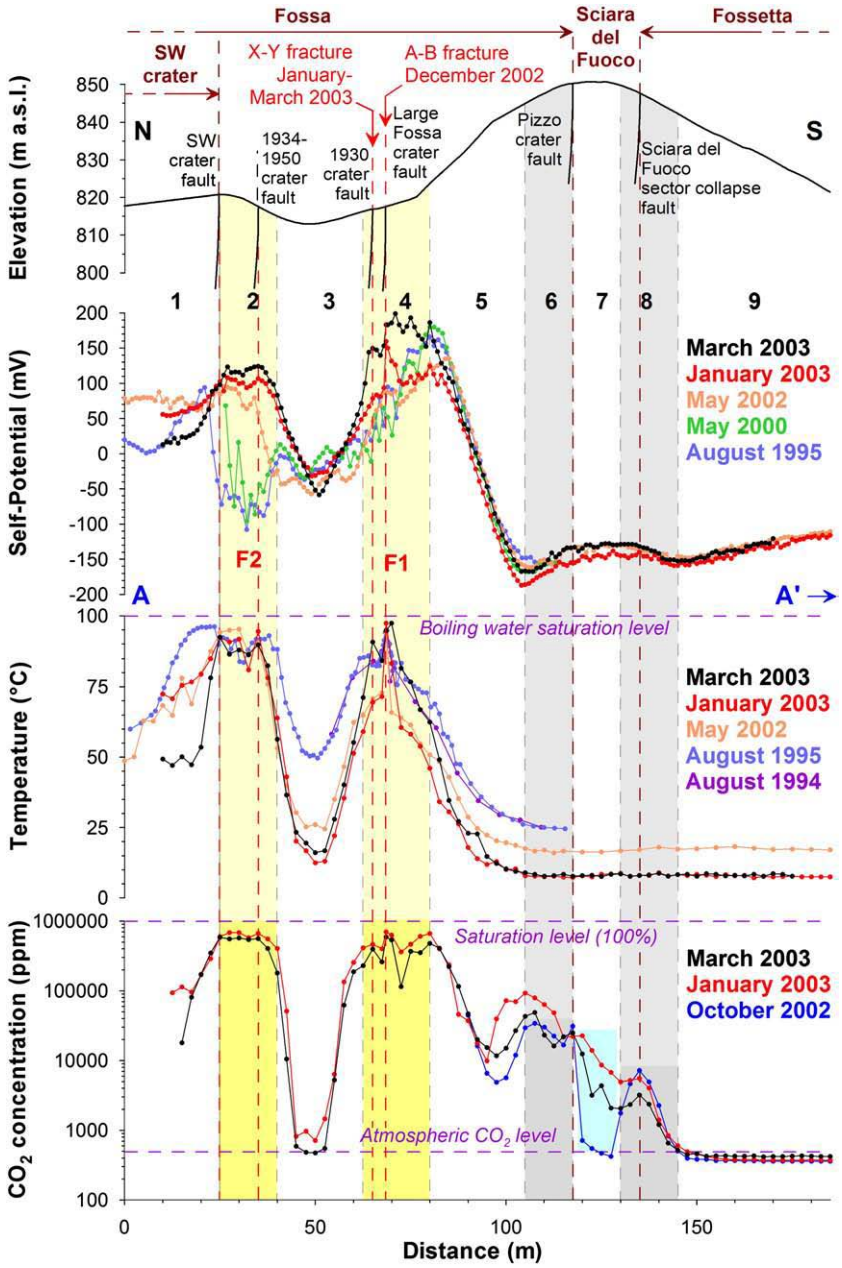

Fig. 6. Reiteration of self-potential, temperature, and CO_2 soil concentration measurements along Profile A–A′ shown in Figs. 1, 2, and 3, before and during the 2002–2003 eruptive crisis. Only the first 185 m of Profile A–A′ (315 m long) has been represented. The reference for the self-potential measurements is located at position A′ of this profile (see Fig. 2).

The stability of the peaks of the CO_2 concentrations over the anomalies F1 and F2 was due to the saturation of the signal. Indeed, the concentration of CO_2 is buffered near saturation. The flux of CO_2 would not have such a drawback and would be therefore more sensitive to in situ changes in the degassing of carbon dioxide. This outlines the limitations of using the concentration rather than the flux of CO_2 to monitor areas of high degassing. However, for areas of lower permeability, such as in Sectors 1 and 3 and in Sectors 5 to 9, the dynamics of the CO_2 concentration can be observed because it is below the saturation of this signal.

5. Interpretation and discussion

The data obtained before and during the 2002–2003 eruptive crisis associated with the permeability increase of the summit area inferred from the propagation of the fracture network during the eruptive crisis, raised three main questions: (1) What are the parameters involved in the genesis of the fracture network across the Fossa area? (2) What changes occurred in fluid flow and heat transfer before the 2002–2003 eruptive crisis? and (3) What changes occurred in the flow of fluids and heat transfer during the 2002–2003 eruptive crisis? The responses to these three questions may help to understand the occurrence of this network of fractures in terms of potential geohazard.

5.1. The fractures across the Fossa area

5.1.1. Analysis of the 2002–2003 fracture network

The opening of a network of fractures across the Fossa area at the beginning of the 2002–2003 eruptive crisis raised the question of the origin of this network. Because the fractures occurred at the beginning of the eruptive crisis, they are likely associated, directly or indirectly, with the two flank failures ($\sim 26 \times 10^6$ m^3) that occurred in the northern part of the Sciara del Fuoco and to the collapses of the NE, Central, and part of the SW craters. The main question we want to discuss first is to know if these fractures are the result of a local deformation or if they are precursory signs of a giant landslide of a major part of the Sciara del Fuoco area (Fig. 1).

The absence of continuity of the fracture network, outside the Fossa area (see Fig. 3), plays in favour of the assumption that these fractures result from the centripetal deformation associated in turn by the internal collapse of the summit craters. However, the location of this network of fractures is not in good agreement with the expect pattern associated with such a collapsed area in a homogeneous material. Indeed, in this case, a collapsed area induces the apparition of a set of bowed normal faults all around the collapsed zone at a distance lower than the radius of the collapsed area (Van Wyk de Vries and Matela, 1998; Roche et al., 2000; Vidal and Merle, 2000; Van Wyk de Vries et al., 2000; Merle et al., 2001; Merle and Lénat, 2003; Acocella et al., 2004). This is obviously not the case here (see Fig. 3). Indeed, in the cold zone for instance, the distance between the inner fractures and the boundary of the collapse area is higher than the diameter of the collapsed area.

In order to explain the large distance from the crater collapse boundary to the fractures, we look for an explanation related to the possibility that the displacements that occurred inside the Fossa area were mainly controlled by structural heterogeneities. These later should be the consequence of old collapse events (faults or ring fault) that occurred in the summit area. This is clearly the case for the fractures A to E, which are located in the southern part of the Fossa area. They coincide indeed with the structural boundary of the Large Fossa crater previously identified by Finizola et al. (2003). This structural boundary divides the Pizzo pyroclastic products from scoria materials (Finizola et al., 2003; Revil et al., 2004). It is therefore obvious that the network of fractures was guided here by the reactivation of the Large Fossa crater fault. The problem is therefore to understand why, further away, from point "E" in Fig. 3, the network of fracture does not follow the Large Fossa crater boundary. One hypothesis is to consider that other structural boundaries also control the occurrence of these fractures in the Fossa area. We provide below a detailed review of the morphological evolution of the Fossa area over the last 70 years. This review reveals that this assumption could be correct.

5.1.2. Comparison between the new fracture network and historical data

Because of its persistent activity over more than thousand years (Mercalli, 1881; Rosi et al., 2000), Stromboli is one of the best documented volcano in the world. Since the middle of the nineteenth century, the explosive activity of Stromboli has been described quite precisely. This activity is characterized by a mild explosive activity disrupted by major and paroxysmal events (Barberi et al., 1993). The strongest paroxysmal event known over the last century occurred in September 11th, 1930. It was responsible for the complete reorganization of the Fossa area (Rittmann, 1931). Sketches made by Rittmann in 1931 before and after this event are shown in Fig. 7A and B. They show the presence of a collapse crater with a depth of several meters located inside the larger structural boundary of the Large Fossa crater. The Large Fossa crater can be easily recognized on the sketches as it divides the Pizzo pyroclastite outcrops from the refilled scoria material (see Fig. 7A and B and Finizola et al., 2003). During the following seventy years, the structural boundary of the Large Fossa crater has been covered by volcanic products with the exception of the western boundary of the outcrops 3, 4, 5, and 6 (see Fig. 3).

Comparison between the position of the 1930 crater boundary located inside the Large Fossa crater (Fig. 7B) and the position of the fractures discussed above suggests strongly that the inner fractures X–Y, T–U, S–H–I, J–K–L, and V–W in Fig. 3 have been guided by the structural boundary of the 1930 collapse crater. With this assumption, the T–U and S–H–I fractures appear as classic parallel collapse fractures while the fractures E–F and G–H may be explained by stress readjustment between the two crater collapse structures.

Since 1931, the morphology of the Fossa has evolved during two distinct periods (see Fig. 7B and C). Between September 1931 and June 1952, the progressive construction of cones of scoria resulting from the typical explosive strombolian activity was disrupted by seven paroxysmal destructive events: (1) in February 2nd, 1934, (2) in January 31st, 1936, (3) in October 26–27th, 1936, (4) in August 22th, 1941, (5) in December 3rd, 1943, (6) in August 20th, 1944, and (7) in October 20–23th, 1950 (Barberi et al., 1993). All these events were characterized by magnitudes that were smaller than the one associated with the September 11th, 1930 paroxysmal event. However, this series of events was responsible for the construction, over 16 years (1934–1950), of a unique collapse crater boundary involving the SW and NE craters (see Fig. 7C and Bullard, 1954). The last important paroxysmal event before the 2002–2003 eruptive crisis occurred in February 1st, 1954 (Barberi et al., 1993). During the fifty following years (1954–2003), mild explosive activity allowed the construction and individualisation of the SW and NE scoria cones. Fig. 8 shows a comparison between the sketch made in 1952 (see Fig. 7C), the picture taken in April 2003 (Fig. 7D), and the temperature map realized in 1999 by Finizola et al. (2003). This comparison shows that the 1934–1950 crater boundary has allowed a preferential fluid migration between the F2 and F5 temperature anomalies since 2003. The paroxysmal event of April 5th, 2003 (Calvari et al., 2006) was responsible for the collapse of the ground between the Central and the NE craters (Fig. 7D).

The sketch map made in 1952 (see Fig. 7C) shows also two open "cracks" in the terminology used by Bullard (1954) in the Fossa area. These two cracks were associated with steam emission. It is tempting to associate these old observations to the T–U and S–H reactivated fractures observed in 2003 (see Fig. 7D).

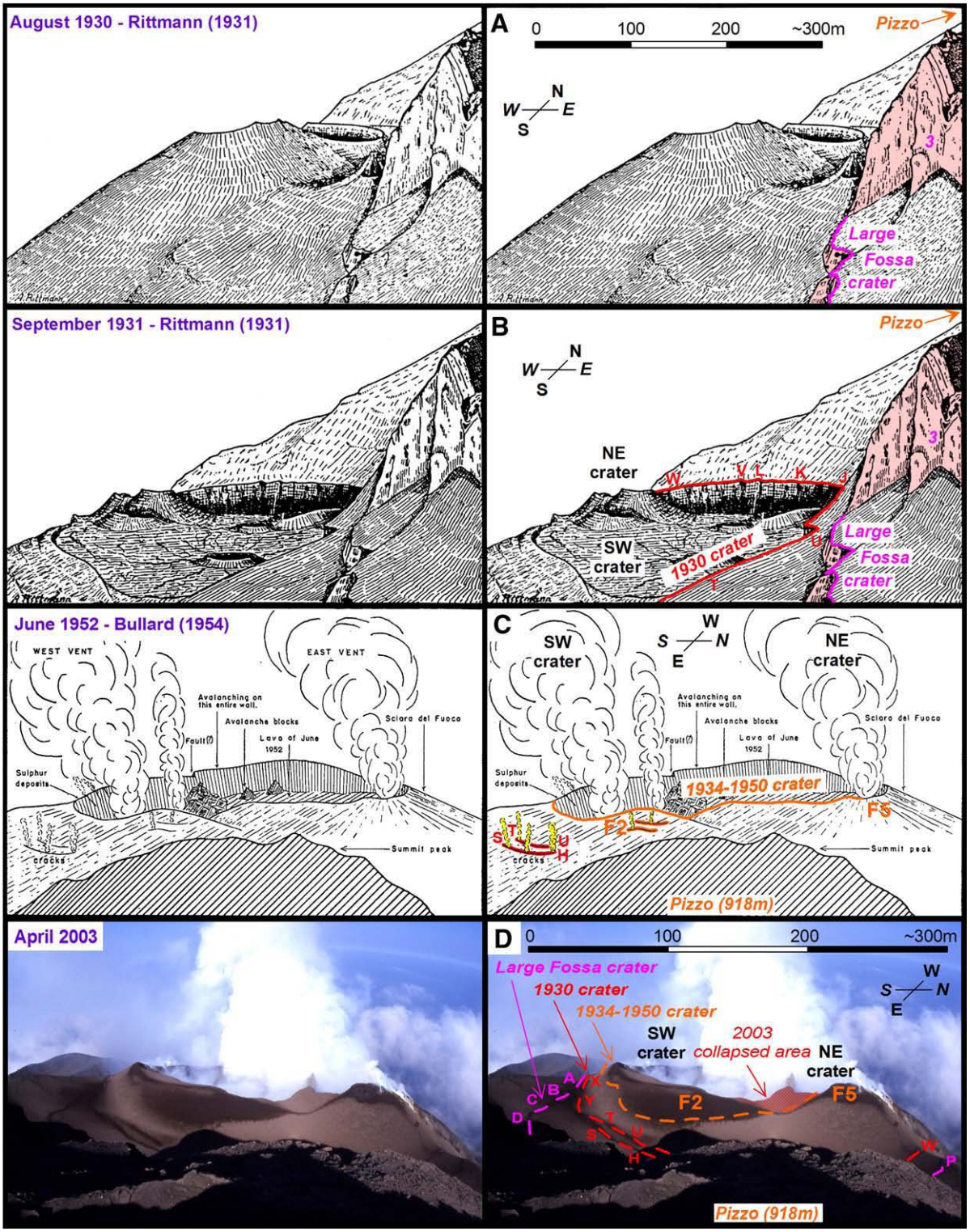

Fig. 7. A, B: Historical sketch map of the Fossa area before and after the largest historical paroxysmal eruption that occurred at Stromboli volcano on September 11th, 1930 (Rittmann, 1931). Panel B shows the morphological consequence of the September 11th, 1930 paroxysm. This paroxysm entirely restructured the morphology of the Large Fossa crater area. C: Sketch of the Fossa area in June 1952 (from Bullard, 1954) showing a unique crater rim between the present-day SW and NE craters. This unique crater rim was reshaped from 1934 to 1950 by seven paroxysmal events (Barberi et al., 1993). The presence of "cracks" was observed in the Fossa area associated with steam. The position of these cracks seems consistent with those encountered during the 2002–2003 eruptive crisis. D: Pictures of the Fossa area on April 2nd 2003, showing the area that collapsed in 2003 between the Central and NE craters along the crater boundary visible in June 1952 (see Fig. 7C, Bullard, 1954) and evidenced in 1999 by the existence of thermal anomalies (see Finizola et al., 2003). The labels of the fractures and other colored symbols are the same as in Figs. 2 and 3. (For interpretation of the references to color in this figure legend, the reader is referred to the web version of this article.)

In summary, the analysis of historical documents from Stromboli suggests that three crater boundaries probably played an important role in the morphological evolution of the Fossa area during the 2002–2003 eruptive crisis (Fig. 8): (1) The Large Fossa crater, (2) the 1930 crater boundaries, and (3) the 1934–1950's crater boundary. Therefore the location of the network of fractures that appeared during the

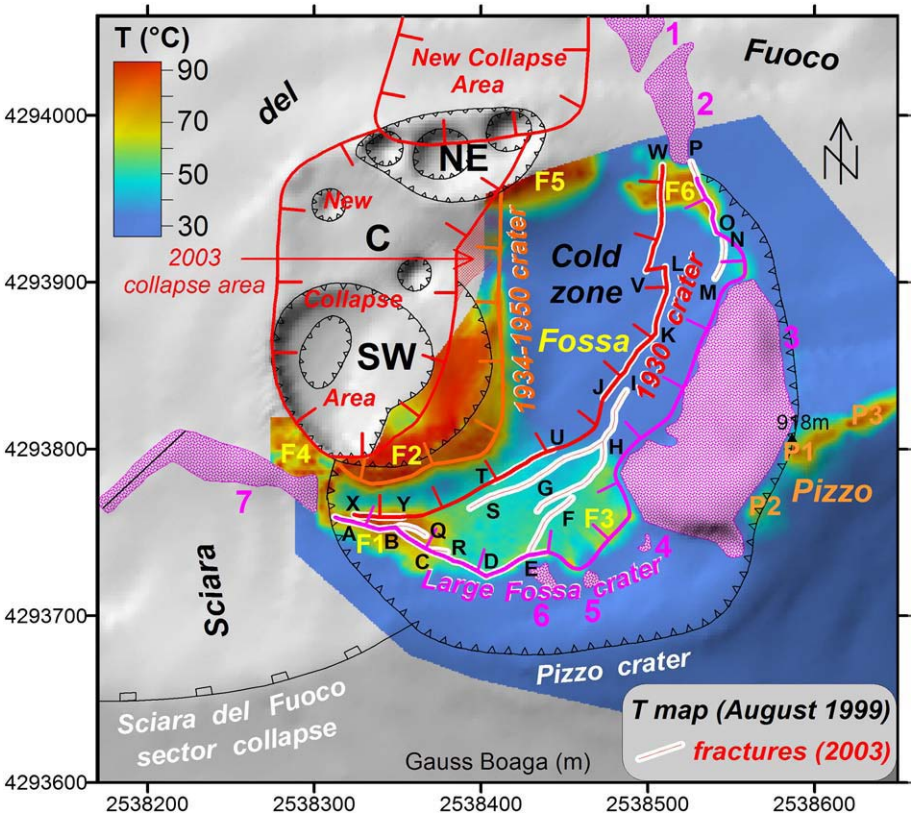

Fig. 8. Correlation between the position of the old structural boundaries and the position of the network of fractures located in the Fossa area during the 2002–2003 eruptive crisis. The geometry of the rims of the Large Fossa crater and the 1934–1950 crater has been determined from self-potential and temperature measurements (see Finizola et al., 2003). The determination of the position of the boundary of the 1930 crater comes from the superposition of the 2002–2003 network of fracture and the sketches made by Rittmann (1931) (see Fig. 7). Note the position of the 2003 collapsed area between the present-day Central and SW crater compared to Fig. 7D. The "cold zone" corresponds likely to the presence of a perched aquifer according to Finizola et al. (2003) and Revil et al. (2004).

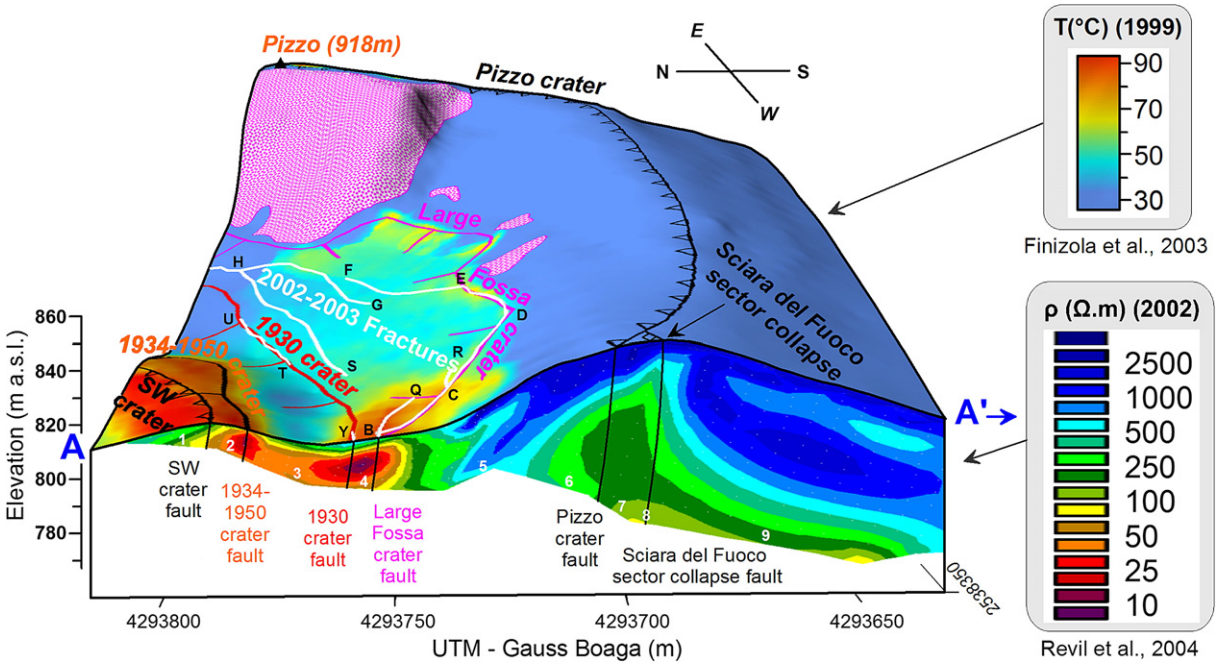

Fig. 9. 3D view of the Fossa area showing the 2D high resolution electric resistivity tomography section performed in May 2002 by Revil et al. (2004). The Sectors 4 and 7 (see Fig. 6) correspond to the 2002–2003 network of fractures in the Fossa area and to the increase of the soil concentrations of CO_2 between the Sciara del Fuoco sector collapse boundary and the Pizzo crater, respectively. These sectors were already identified in May 2002, 7 months before the beginning of the 2002–2003 eruptive crisis, thanks to the inverted resistivity cross-sections. On these cross-sections, these sectors were associated with two major electric resistivity discontinuities. The labels 1 to 9 (in white) represent the different sectors of fluid flow identified along Profile A–A′. They are also shown on Figs. 3, 6 and commented in the text. Labels B to Y allow locating these fractures on Figs. 2, 3, 7 and 8.

2002–2003 Stromboli eruptive crisis does not play in favour for a potential reactivation of the Sciara del Fuoco sector collapse area.

During the 2002–2003 eruptive crisis, only the permeability of the Large Fossa (F1, F3 and F6 anomalies) and the 1934–1950's crater boundaries (continuity between F2 and F5 anomalies) were high enough to allow a preferential migration of fluids. Previous studies (Finizola et al., 2003; Revil et al., 2004) showed that the Fossa area is crossed by a drainage network of water flows coming from the condensation of the water vapour close to the ground surface where the anomalies F1, F2, F3, F5 and F6 are located. This shallow drainage network crosses the 1930's crater rim. It drags water from the position of the thermal anomalies toward the cold zone of the Fossa area, which was interpreted by Revil et al. (2004) to be a perched aquifer. Therefore, we can hypothesized that the 1930's crater rim cannot be detected with thermal anomalies because this crater rim has been sealed at a shallow depth probably comprised between 5 and 10 m (see Finizola et al., 2003; Revil et al., 2004).

The consideration of these three crater boundaries in dragging preferential fluid rising systems also allows better interpretation of the detailed self-potential and temperature signal variation along Profile A–A′, with slight increase of the signals in agreement with the position of these structural boundaries (Fig. 6). This result supports the presence of two preferential crater boundaries constituting the SW crater cone (the SW and the 1934–1950 crater rims, see Finizola et al. (2003)).

Fig. 9 shows the superposition (1) of the ground temperature data made in 1999, (2) the high resolution electric resistivity tomography carried out along Profile A–A′ in May 2002 before the eruptive crisis (data from Revil et al., 2004 have been improved in this figure, reprocessing the data with a precise digital elevation model and using a high number of iterations) (3) the fracture network that opened during the 2002–2003 eruptive crisis. This figure shows that the two areas that played a major role during the eruptive crisis correspond both to strong contrasts of the resistivity at shallow depths (see Sector 4 with the 2002–2003 fractures and Sector 7 between the southern Sciara del Fuoco boundary and the Pizzo crater on Figs. 6 and 9). Low resistivity values are associated with the ascent of hot hydrothermal fluids probably in a network of open cracks. These open cracks not only favour the migration of warm fluids but there are also mechanically weak domains as evidenced by the occurrence of fractures during the eruptive crisis. The use of electrical resistivity tomography represents therefore a powerful method to identify mechanically weak areas that may correspond to sliding planes for landslides during a volcanic crisis.

5.2. Changes in fluid flow and heat transfer along the summit fractures prior the eruptive crisis

The signals measured before the 2002–2003 eruptive crisis (Fig. 6) exhibit two striking features: (1) the F2 self-potential anomaly shows a transition from a minimum in August 1995 to May 2000 to a maximum from May 2002 to March 2003. (2) The width of the F1 and F2 temperature anomalies (Sector 3 and 5 in Fig. 6) showed a significant decrease from August 1994 to August 1995 and from May 2002 to March 2003. These observations imply strong changes in fluid flow and heat transfer during the period from May 2000 to May 2002, so before the eruptive crisis. In order to explain the change observed in the F2 self-potential anomaly, we suggest an inversion in the direction of the flow of the ground water. From August 1995 to May 2000, a preferential water infiltration system was proposed along this structural boundary to be responsible for the self-potential minimum (see Finizola et al., 2003, Revil et al., 2004). Since May 2002, the increase of the self-potential signals is likely related to the upwelling of hydrothermal fluids in this area. Such a change in the pattern of ground water flow could be the consequence of an increase of the permeability along this structural boundary between May 2000 and May 2002.

The assumption of a permeability increase along the structural boundaries associated with the anomalies F1 and F2 may also explain the decrease of the width of the F1 and F2 temperature anomalies observed after the May 2000–May 2002 period. Considering indeed that the temperature distribution is both influenced by advection of hot fluids and by the condensation of the steam (Chiodini et al., 2005), an increase of permeability would involve an increase of the heat flux towards the surface. But, above a threshold of permeability, part of the advection can reach the surface and the atmosphere, and in this case, the energy coming from steam condensation will be released outside of the soil and will not heat the system. In this case, the width of the temperature anomalies associated with a major upwelling of hot fluids would be smaller and the temperature minimum between the two anomalies would be lower because part of the steam condensation energy is lost in the atmosphere. It follows that an increase of the permeability along the anomalies F1 and F2, and between May 2000 and May 2002 can explain both the self-potential and temperature changes observed after this period. Moreover, this assumption is compatible with the opening of the network of fractures observed 300 m lower, in the Sciara del Fuoco area, between November 2000 and April 2001 and showing over 45 cm of pure extensional displacement (Tibaldi et al., 2003). These events revealed before the 2002–2003 eruptive crisis, the importance of the instability processes occurring in the upper southern part of the Sciara del Fuoco area.

5.3. Changes in fluid flow and heat transfer along the summit fractures during the eruptive crisis

The reiteration of self-potential, temperature, and CO_2 soil-gas measurements along Profile A–A′ allows a better understanding of the complexity of the parameters involved in the morphological changes that occurred during the 2002–2003 eruptive crisis. The most striking result obtained by using simultaneously these three methods is that the different information does not always reveal the same spatio-temporal variations. Considering that all of the methods are sensitive to the flow of pore fluids (water and gas), the main problem is therefore to understand why there are such differences in the change of these parameters and what information can be extracted from these changes.

During the eruptive crisis, three geographic areas with high variations of the self-potential, temperature, and/or CO_2 soil-gas signal were observed (see their positions in Fig. 6). They are (1) Sector 7, corresponding to the southern present morphology of the Sciara del Fuoco, (2) Sectors 4 and 2 corresponding to the fracture area and to the upper external flank of the SW crater, respectively, and (3) Sector 1 corresponding to the inner flank of the SW crater. In Sector 7, the present southern morphology of the Sciara del Fuoco is interpreted as resulting from a relatively small failure (Tibaldi, 2001; Tibaldi et al., 2003; Apuani et al., 2005a,b). Obviously, the geometry of this entire sliding surface is of a major importance in term of volume and extension of this potential collapse zone. Only the interpretation of a deep electrical resistivity tomography crossing the Sciara del Fuoco area could give the geometry of this potential sliding plane.

5.3.1. Changes in Sector 7

In January 2003, Sector 7 exhibits a drastic increase in the soil concentration of the CO_2 in comparison with the measurements performed in October, 2002. However this period did not show any concomitant significant changes in the self-potential and temperature signals. As we are dealing with CO_2 concentration and not fluxes, two assumptions can be suggested to explain these observations. The former corresponds to an increase in the concentration CO_2 in the magmatic source. The second possibility corresponds to a constant source but is related to an increase of the permeability in Sector 7. The

first assumption can be dismissed right away because an increase in the concentration of CO_2 from a magmatic source would affect the neighbouring Sectors 7 and 8. No increases in CO_2 signal were observed in Sector 8 between October 2002 and January 2003 despite its high permeability. Therefore, the increase of the CO_2 concentration between the Sciara del Fuoco sector collapse and the Pizzo crater can only be explained by an increase of the permeability in this area. This suggests that the southern sector collapse area of the Sciara del Fuoco (crossing the profile A–A′) has probably been slightly affected by the two collapses that occurred in the northern part of the Sciara del Fuoco on December 30th, 2002 (Fig. 1). An increase of the concentration of CO_2 in this area agrees also with the opening of the fractures between November, 2000 and April, 2001 (Tibaldi et al., 2003). This is at ~300 m below Sector 7 where the change of permeability was observed along Profile A–A′ (Fig. 1). Therefore, it appears that both the northern and southern parts of the Sciara del Fuoco were affected by gravitational instability. To monitor this instability in the upper southern part of the Sciara del Fuoco area, one permanent GPS station was installed just below the fractures evidenced by Tibaldi et al. (2003) (see Puglisi et al., 2005 and Fig. 1). This was done at the beginning of the eruptive crisis.

The data acquired in March 2003 show a slight decrease in the concentration of CO_2 along the entire profile and especially in Sector 7. This observation can be interpreted as a lower input of CO_2 through the plumbing system of the volcano. At the opposite, it is not consistent with a sealing effect occurring at depth that would decrease the influx of carbon dioxide. Indeed, in Sectors 2 and 4 for instance, the concentration of CO_2 decreases while variations in the self-potential, temperature, and faulting are consistent with an increase of the permeability in these sectors. This hypothesis of a lower input of CO_2 between January and March 2003 can find an explanation from the fact that the effusion that appeared in the Sciara del Fuoco area on February 15th 2003 (Calvari et al., 2006) also dragged the volcanic gases decreasing the influx of carbon dioxide in the summit area.

In Sector 7, the self-potential and temperature data show no significant change before and during the eruptive crisis. This suggests that the increase of the permeability was high enough to allow higher gas flux transfer, but not sufficient to allow higher hydrothermal flow rates in this area. Indeed, for low permeability areas, gases are more mobile than water.

5.3.2. Changes in Sectors 2 and 4

Since January 2003, Sectors 2 and 4 showed a sharp increase in the self-potential data, reaching the highest values (about +200 mV) in March 2003. This result agrees with the general lengthening of the fracture system in the Fossa area observed between January and April, 2003 (Fig. 3). Fracturing is associated with an increase of the permeability during the first months of the eruptive crisis. This permeability increase is in turn associated with a sharp increase of the fumarolic activity over the highest temperature areas of the fracture network. The increase of the flux of the pore water was also responsible for higher amplitudes of the streaming potentials along the fracture network. The fractures of the anomaly F1 (see location in Fig. 6) exhibit an increase of the amplitude of the self-potential signals during the eruptive crisis. The same is true for the anomaly F2 (see Fig. 6) despite the fact that this anomaly has not been affected at the ground surface by a visible network of fractures. This increase in the amplitude of self-potential signal between January and March 2003 could be interpreted as the consequence of the increase in the fumarolic activity observed along the fracture network, dragging therefore more electrical charges toward the surface. As described in Section 5.1, the anomalies F1 and F2 are supposed to contain a double fracture system related (1) the Large Fossa crater and the 1930's crater boundary and (2) the 1934–1950's crater and SW crater boundary (Figs. 6 and 9). It can be therefore hypothesized that during the first months of the eruptive crisis, the permeability increased along all of these limits.

We note that while self-potential data anomalies increased in magnitude, the maxima in the temperature distribution did not display any significant variation for the same F1 and F2 anomalies. This absence of increase is well-explained by the fact that the temperature does not exceed the boiling point of water.

The temperature and CO_2 maps of January and April 2003 (see Fig. 4) show that the migration of the temperature along the fracture system was slower than the migration of the CO_2 signal. Indeed, by January 2003 the values of CO_2 (Fig. 4B) were already high and very similar to those of April 2003 (Fig. 4D), whereas for the temperature maps, a significant temperature increase was observed between January 2003 (Fig. 4A) and April 2003 (Fig. 4C). This observation is consistent with the fact that the thermal diffusivity is much smaller than the diffusivity associated with the transport of carbon dioxide (Chiodini et al., 2005).

5.3.3. Changes in Sector 1

From January to March 2003, we also observed a sharp decrease in the values of the self-potential and temperature inside the SW crater (see Sector "1" in Fig. 6). This observation is likely related to the cooling of the SW crater because of the descent of the magma (the heat source) inside the conduits to sustain lower-elevation lava flows associated with the effusion of the magma in the Sciara del Fuoco area (Fig. 1).

In terms of evaluating the occurrence of a possible landslide, this means that the southern Sciara del Fuoco area has been only slightly affected by the eruptive crisis. The higher permeability deduced from the data of January 2003 stopped increasing in the southern Sciara del Fuoco area at that time while the fracturation of the Fossa area remained active from January to March 2003. The evolution of the permeability of the structural boundaries in the summit area, during the first months of the eruptive crisis, implies that the most probable collapse event was related to the collapse of old crater boundaries inside the Fossa area. The possibility of a flank destabilization of the entire Sciara del Fuoco area was therefore unlikely for this eruptive crisis. This is the main finding of the present work. This hypothesis is also in good agreement with the March 15th, 2007 eruptive crisis of Stromboli, which induced a vertical collapse of the summit crater area (Neri and Lanzafame, 2008).

6. Conclusion

Combining electric resistivity tomography, self-potential, temperature, and the measurement of the soil CO_2 concentration represents a powerful approach to follow the dynamics of fluids flow along faults and fractures in a volcanic edifice. These methods applied before and during the 2002–2003 Stromboli eruptive crisis show the complex structural pattern of the Fossa area in terms of old structural boundaries playing a prominent part in the opening of a new network of fractures and the concomitant collapse of several areas. The data collected before the 2002–2003 eruptive crisis allows to infer the most permeable areas of this system. These permeable pathways are also interpreted as mechanically weak areas. These weak zones evolved in open fractures during the eruptive crisis. Self-potential, temperature, and CO_2 concentration techniques also showed permeability changes during the eruptive crisis, and the related disruptions in the channelling of the ground water along several structural boundaries. In terms of potential volcanic hazard, the evolution of these structural boundaries, during the first months of the eruptive crisis, suggests that the most probable collapse event would be related to the collapse of old crater boundaries inside the Fossa area rather than a possible destabilization of the Sciara del Fuoco area. This hypothesis has been confirmed in 2007 by a new eruptive crisis that reached the collapse of a large part of the Fossa area. The increase of the permeability of the

southern part of the Sciara del Fuoco sector collapse area, at the beginning of the 2002–2003 eruptive crisis, and the potential consequences of such a giant landslide in terms of tsunami generation affecting all of the Tyrrhenian sea coasts, suggest the need for a permanent monitoring system in this area. The identification of strategic areas to install permanent monitoring systems, where the signal amplitude variation is significant during an eruptive crisis, needs previous detailed mapping and accessibility of the upper part of a volcano using these different techniques. Therefore, electric resistivity tomography, self-potential, temperature, and soil-gas measurements offer a powerful tool in locating the structural discontinuities inside the volcanic edifice involving differential fluid flow pathways useful to assess potential collapses associated with fault planes.

Acknowledgements

We are grateful to the Italian Civil Protection Institute for their support with the use of the Air Walser helicopter during the 2002–2003 eruptive crisis. The three field campaigns carried out in 2003 have been supported by funding from the Italian Civil Protection Institute. A. F. acknowledges the "Conseil Régional d'Auvergne" in France for a research grant during the 2002–2003 period, and thanks Jean Todt (sports director of Formula One Scuderia Ferrari), Giancarlo Minardi (director of the Minardi Formula One team), Flavio Briatore (ex-director of the Formula One Benetton team), and Marc Demougeot (director of Sparco-France) for their help into obtaining Formula One fireproof equipment. Without it, measurements near the active craters during the 2002–2003 eruptive crises could not have been performed for security reasons. The authors wish to thank Alessandro Tibaldi, Nicolas Fournier, and James Cowlyn for earlier corrections of this manuscript. Nicolas Coppo and an anonymous reviewer are also sincerely thanked for their very constructive comments. This is IPGP contribution number 2486.

References

Acocella, V., Funiciello, R., Marotta, E., Orsi, G., de Vita, S., 2004. The role of extensional structures on experimental calderas and resurgence. J. Volcanol. Geotherm. Res. 129 (1–3), 199–217. doi:10.1016/S0377-0273(03)00240-3.

Aizawa, K., Uyeshima, M., Nogami, K., 2008. Zeta potential estimation of volcanic rocks on 11 island arc-type volcanoes in Japan: implication for the generation of local self-potential anomalies. J. Geophys. Res. 113, B02201. doi:10.1029/2007JB005058.

Apuani, T., Corazzato, C., Cancelli, A., Tibaldi, A., 2005a. Stability of a collapsing volcano (Stromboli, Italy): limit equilibrium analysis and numerical modelling. J. Volcanol. Geotherm. Res. 144 (1–4), 191–210. doi:10.1016/j.jvolgeores.2004.11.028.

Apuani, T., Corazzato, C., Cancelli, A., Tibaldi, A., 2005b. Physical and mechanical properties of rock masses at Stromboli: a dataset for volcano instability evaluation. Bull. Eng. Geol. Environ. 64 (4), 419–431. doi:10.1007/s10064005-0007-0.

Aubert, M., 1999. Practical evaluation of steady heat discharge from dormant active volcanoes: case study of Vulcarolo fissure (Mount Etna, Italy). J. Volcanol. Geotherm. Res. 92, 413–429.

Aubert, M., Kieffer, G., 1984. Evolution d'une intrusion magmatique dans le flanc sud de l'Etna entre juin 1982 et juin 1983. Résultats de potentiel spontané (PS) et essai d'interprétation de l'éruption de 1983. C. R. Acad. Sci. Paris t.296, 379–382 Série II-8.

Aubert, M., Lima, E., 1986. Hydrothermal activity detected by self-potential measurements (SP) at the N–S volcanic axis between the volcanoes "Nevado de Colima" and "Fuego de Colima", Mexico. Geophys. J. Int. 25–4, 575–586.

Aubert, M., Baubron, J.C., 1988. Identification of a hidden thermal fissure in a volcanic terrain using a combination of hydrothermal convection indicators and soil-atmosphere analysis. J. Volcanol. Geotherm. Res. 35, 217–225.

Aubert, M., Auby, R., Bourley, F., Bourley, Y., 1984. Contribution à la surveillance de l'activité de l'Etna à partir de l'étude des zones fumeroliennes. Bull. Volcanol. 47, 1039–1050.

Baldi, P., Fabris, M., Marsella, M., Monticelli, R., 2005. Monitoring the morphological evolution of the Sciara del Fuoco during the 2002–2003 Stromboli eruption using multi-temporal photogrammetry. J. Photogram. Rem. Sens. 59 (4), 199–211. doi:10.1016/j.isprsjprs.2005.02.004.

Ballestracci, R., 1982. Self-potential survey near the craters of Stromboli volcano (Italy). Inference for internal structure and eruption mechanism. Bull. Volcanol. 45, 349–365.

Barberi, F., Rosi, M., Sodi, A., 1993. Volcanic hazard assessment at Stromboli based on review of historical data. Acta Vulcanol. 3, 173–187.

Bertagnini, A., Landi, P., 1996. The Secche di Lazzaro pyroclastics of Stromboli volcano: a phreatomagmatic eruption related to the Sciara del Fuoco sector collapse. Bull. Volcanol. 58, 239–245.

Bolève, A., Revil, A., Janod, F., Mattiuzzo, J.L., Jardani, A., 2007. Forward modeling and validation of a new formulation to compute self-potential signals associated with ground water flow. Hydrol. Earth Syst. Sci. 11 (5), 1661–1671.

Bonaccorso, A., Calvari, S., Garfì, G., Lodato, L., Patanè, D., 2003. Dynamics of the December 2002 flank failure and tsunami at Stromboli volcano inferred by volcanological and geophysical observations. Geophys. Res. Lett. 30 (18), 1941. doi:10.1029/2003GL017702.

Bullard, F.M., 1954. Activity of Stromboli in June and December 1952. Bull. Volcanol. 15, 91–98.

Calvari, S., Spampinato, L., Lodato, L., Harris, A.J.L., Patrick, M.R., Dehn, J., Burton, M.R., Andronico, D., 2005. Chronology and complex volcanic processes during the 2002–2003 flank eruption at Stromboli volcano (Italy) reconstructed from direct observations and surveys with a handheld thermal camera. J. Geophys. Res. 110, B02201. doi:10.1029/2004JB003129.

Calvari, S., Spampinato, L., Lodato, L., 2006. The 5 April 2003 vulcanian paroxysmal explosion at Stromboli volcano (Italy) from field observations and thermal data. J. Volcanol. Geotherm. Res. 149, 160–175. doi:10.1016/j.jvolgeores.2005.06.006.

Carapezza, M.L., Federico, C., 2000. The contribution of fluid geochemistry to the volcano monitoring of Stromboli. J. Volcanol. Geotherm. Res. 95, 227–245.

Chiocci, F.L., Romagnoli, C., Tommasi, P., Bosman, A., 2008. The Stromboli 2002 tsunamigenic submarine slide: characteristics and possible failure mechanisms. J. Geophys. Res. 113, B10102. doi:10.1029/2007JB005172.

Chiodini, G., Granieri, D., Avino, R., Caliro, S., Costa, A., Werner, C., 2005. Carbon dioxide diffuse degassing and estimation of heat release from volcanic and hydrothermal systems. J. Geophys. Res. 110, B08204. doi:10.1029/2004JB003542.

Crespy, A., Bolève, A., Revil, A., 2007. Influence of the Dukhin and Reynolds numbers on the apparent zeta potential of granular media. J. Colloid Interface Sci. 305, 188–194.

Etiope, G., Beneduce, P., Calcara, M., Favali, P., Frugoni, F., Schiattarella, M., Smriglio, G., 1999. Structural pattern and CO_2–CH_4 degassing of Ustica Island, Southern Tyrrhenian basin. J. Volcanol. Geotherm. Res. 88, 291–304.

Finizola, A., Sortino, F., Lénat, J.F., Valenza, M., 2002. Fluid circulation at Stromboli volcano, (Aeolian Island, Italy) from self-potential and CO_2 surveys. J. Volcanol. Geotherm. Res. 116 (1–2), 1–18.

Finizola, A., Sortino, F., Lénat, J.F., Aubert, M., Ripepe, M., Valenza, M., 2003. The summit hydrothermal system of Stromboli: new insights from self-potential, temperature, CO_2 and fumarolic fluids measurements, with structural and monitoring implications. Bull. Volcanol. 65, 486–504. doi:10.1007/s00445-003-0276-2.

Finizola, A., Lénat, J.F., Macedo, O., Ramos, D., Thouret, J.C., Sortino, F., 2004. Fluid circulation and structural discontinuities inside Misti volcano (Peru) inferred from self-potential measurements. J. Volcanol. Geotherm. Res. 135, 343–360. doi:10.1016/j.jvolgeores.2004.03.009.

Finizola, A., Revil, A., Rizzo, E., Piscitelli, S., Ricci, T., Morin, J., Angeletti, B., Mocochain, L., Sortino, F., 2006. Hydrogeological insights at Stromboli volcano (Italy) from geoelectrical, temperature, and CO_2 soil degassing investigations. Geophys. Res. Lett. 33, L17304. doi:10.1029/2006GL026842.

Guichet, X., Jouniaux, L., Catel, N., 2006. Modification of streaming potential by precipitation of calcite in a sand-water system: laboratory measurements pH range from 4 to 12. Geophys. J. Int. 166, 445–460. doi:10.1111/j.1365-246X.2006.02922.x.

Hase, H., Ishido, T., Takakura, S., Hashimoto, T., Sato, K., Tanaka, Y., 2003. ζ potential measurement of volcanic rocks from Aso caldera. Geophys. Res. Lett. 30 (23), 2210. doi:10.1029/2003GL018694.

Hornig-Kjarsgaard, I., Keller, J., Koberski, U., Stadlbauer, E., Francalanci, L., Lenhart, R., 1993. Geology, stratigraphy and volcanological evolution of the island of Stromboli, Aeolian Arc, Italy. Acta Vulcanol. 3, 21–68.

Ishido, T., 2004. Electrokinetic mechanism for the "W"-shaped self-potential profile on volcanoes. Geophys. Res. Lett. 31, L15616. doi:10.1029/2004GL020409.

Lénat, J.F., Robineau, B., Durand, S., Bachélery, P., 1998. Etude de la zone sommitale du volcan Karthala (Grande Comore) par polarisation spontanée. C. R. Acad. Sci. 327, 781–788.

Lewicki, J.L., Connor, C., St-Amand, K., Stix, J., Spinner, W., 2003. Self-potential, soil CO_2 flux, and temperature on Masaya volcano, Nicaragua. Geophys. Res. Lett. 30 (15), 1–4. doi:10.1029/2003GL017731 1817.

Linde, N., Jougnot, D., Revil, A., Matthaï, S.K., Arora, T., Renard, D., Doussan, C., 2007. Streaming current generation in two-phase flow conditions. Geophys. Res. Lett. 34 (3), L03306. doi:10.1029/2006GL028878.

Lorne, B., Perrier, F., Avouac, J.P., 1999a. Streaming potential measurements, 1, properties of the electrical double layer from crushed rock samples. J. Geophys. Res. 104, 17,857–17,877.

Lorne, B., Perrier, F., Avouac, J.P., 1999b. Streaming potential measurements, 2, relationship between electrical and hydraulic flow patterns from rock samples during deformation. J. Geophys. Res. 104, 17,879–17,896.

Malengreau, B., Lénat, J.F., Bonneville, A., 1994. Cartographie et surveillance temporelle des anomalies de Polarisation Spontanée (PS) sur le Piton de la Fournaise. Bull. Soc. Geol. Fr. 165, 221–232.

Maramai, A., Graziani, L., Alessio, G., Burrato, P., Colini, L., Cucci, L., Nappi, R., Nardi, A., Vilardo, G., 2005. Near-and far-field survey report of the 30 December 2002 Stromboli (Southern Italy) tsunami. Mar. Geol. 215 (1–2), 93–106. doi:10.1016/j.margeo.2004.11.009.

Matsushima, N., Michiwaki, M., Okazaki, N., Ichikawa, N., Takagi, A., Nishida, Y., Mori, H.Y., 1990. Self-potential study in volcanic areas — Usu, Hokkaido Komaga-take and Me-akan. J. Fac. Sci. Hokkaido Univ. Ser VII 8, 465–477.

Mercalli, G., 1881. Natura delle eruzioni dello Stromboli ed in generale dell'attività sismo-vulcanica delle Isole Eolie. Atti Soc. It. Sc. Nat. 24, 105–134.

Merle, O., Lénat, J.F., 2003. Hybrid collapse mechanism at Piton de la Fournaise volcano, Reunion Island, Indian Ocean. J. Geophys. Res. 108 (B3), 2166. doi:10.1029/2002JB002014.
Merle, O., Vidal, N., Van Wyk de Vries, B., 2001. Experiments on vertical basement fault reactivation below volcanoes. J. Geophys. Res. 106, 2153–2162.
Neri, M., Lanzafame, G., 2008. Structural features of the 2007 Stromboli eruption. J. Volcanol. Geotherm. Res. doi:10.1016/j.jvolgeores.2008.07.021.
Nishida, Y., Tomiya, H., 1987. Self-potential studies in volcanic areas — Usu volcano. J. Fac. Sci. Hakkaiodo Univ. Ser VII. 8, 173–190.
Porreca, M., Giordano, G., Mattei, M., Musacchio, P., 2006. Evidence of two Holocene phreatomagmatic eruptions at Stromboli volcano (Aeolian Islands) from paleomagnetic data. Geophys. Res. Lett. 33, L21316. doi:10.1029/2006GL027575.
Puglisi, G., Bonaccorso, A., Mattia, M., Aloisi, M., Bonforte, A., Campisi, O., Cantarero, M., Falzone, G., Puglisi, B., Rossi, M., 2005. New integrated geodetic monitoring system at Stromboli volcano (Italy). Eng. Geol. 79 (1–2), 13–31.
Revil, A., Pezard, P.A., Glover, P.W.J., 1999a. Streaming potential in porous media. 1. Theory of the zeta potential. J. Geophys. Res. 104, 20,021–20,031.
Revil, A., Schwaeger, H., Cathles, L.M., Manhardt, P.D., 1999b. Streaming potential in porous media. 2. Theory and application to geothermal systems. J. Geophys. Res. 104, 20,033–20,048.
Revil, A., Leroy, P., 2001. Hydroelectric coupling in a clayey material. Geophys. Res. Lett. 28, 1643–1646.
Revil, A., Linde, N., 2006. Chemico-electromechanical coupling in microporous media. J. Colloid Interface Sci. 302, 682–694. doi:10.1016/j.jcis.2006.06.051.
Revil, A., Naudet, V., Nouzaret, J., Pessel, M., 2003a. Principles of electrography applied to self-potential electrokinetic sources and hydrogeological applications. Water Resour. Res. 39 (5), 1114. doi:10.1029/2001WR000916.
Revil, A., Saracco, G., Labazuy, P., 2003b. The volcano-electric effect. J. Geophys. Res. 108 (B5), 2251. doi:10.1029/2002JB001835.
Revil, A., Finizola, A., Sortino, F., Ripepe, M., 2004. Geophysical investigations at Stromboli volcano, Italy: implications for ground water flow and paroxysmal activity. Geophys. J. Int. 157, 426–440. doi:10.1111/j.1365-246X.2004.02181.x.
Revil, A., Linde, N., Cerepi, A., Jougnot, D., Matthäi, S., Finsterle, S., 2007. Electrokinetic coupling in unsaturated porous media. J. Colloid Interface Sci. 313 (1), 315–327. doi:10.1016/j.jcis.2007.03.037.
Rittmann, A., 1931. Der Ausbruch des Stromboli am 11 September 1930. Zeits. Vulkanol. 14, 47–77.
Roche, O., Druitt, T.H., Merle, O., 2000. Experimental study of caldera formation. J. Geophys. Res., B, Solid Earth Planets 105 (1), 395–416.
Rosi, M., Bertagnini, A., Landi, P., 2000. Onset of the persistent activity at Stromboli volcano (Italy). Bull. Volcanol. 62, 294–300.
Tibaldi, A., 2001. Multiple sector collapse at Stromboli volcano, Italy: how they work. Bull. Volcanol. 63, 112–125.
Tibaldi, A., Corazzato, C., Apuani, T., Cancelli, A., 2003. Deformation at Stromboli volcano (Italy) revealed by rock mechanics and structural geology. Tectonophys 361, 187–204. doi:10.1016/S0040-1951(02)00589-9.
Tinti, S., Pagnoni, G., Zaniboni, F., Bortolucci, E., 2003. Tsunami generation in Stromboli island and impact on the south-east Tyrrhenian coasts. Nat. Hazards Earth Syst. Sci. 3, 1–11.
Tommasi, P., Baldi, P., Chiocci, F.L., Coltelli, M., Marsella, M., Pompilio, M., Romagnoli, C., 2005. The landslide sequence induced by the 2002 eruption at Stromboli volcano. In: Sassa, K., Fukuoka, H., Wang, F., Wang, G. (Eds.), Landslides Risk Analysis and Sustainable Disaster Management, pp. 251–258. doi:10.1007/3-540-28680-2_32.
Van Wyk de Vries, B., Matela, R., 1998. Styles of volcano-induced deformation: numerical models of substratum flexure, spreading and extrusion. J. Volcanol. Geotherm. Res. 81, 1–18.
Van Wyk de Vries, B., Kerle, N., Petley, D., 2000. Sector collapse forming at Casita Volcano, Nicaragua. Geology 28 (2), 167–170.
Vidal, N., Merle, O., 2000. Reactivation of basement faults beneath volcanoes; a new model of flank collapse. J. Volcanol. Geotherm. Res. 99 (1–4), 9–26.
Zablocki, C.J., 1976. Mapping thermal anomalies on an active volcano by the self-potential method, Kilauea, Hawaii. Proceedings, 2nd U N Symposium of the development and use of geothermal resources San Francisco California, May 1975, pp. 1299–1309.
Zlotnicki, J., Nishida, Y., 2003. Review on morphological insights of self-potential anomalies on volcanoes. Surv. Geophys. 24, 291–338. doi:10.1023/B:GEOP.0000004188.67923.ac.